Published in final edited form as:
Biomaterials. 2007 December ; 28(35): 5271–5279. doi:10.1016/j.biomaterials.2007.08.008.

Silk fibroin microtubes for blood vessel engineering

Michael L. Lovett[a], **Christopher Cannizzaro**[a,b], **Laurence Daheron**[c,d], **Brady Messmer**[a], **Gordana Vunjak-Novakovic**[e], and **David L. Kaplan**[a,*]

a *Department of Biomedical Engineering, Tufts University, 4 Colby St., Medford, MA 02155, USA*

b *Harvard-MIT Division for Health Sciences and Technology, Massachusetts Institute of Technology, 77, Massachusetts Ave., E25-519, Cambridge, MA 02139, USA*

c *Center for Regenerative Medicine, Massachusetts General Hospital, Harvard Medical School, CPZN-Room 4400, 185 Cambridge St., Boston, MA 02114, USA*

d *Harvard Stem Cell Institute, 42 Church St., Cambridge, MA 02138, USA*

e *Department of Biomedical Engineering, Columbia University, 351 Engineering Terrace, 1210 Amsterdam Ave., MC 8904, New York, NY 10027, USA*

Abstract

Currently available synthetic grafts demonstrate moderate success at the macrovascular level, but fail at the microvascular scale (<6 mm inner diameter). We report on the development of silk fibroin microtubes for blood vessel repair with several advantages over existing scaffold materials/designs. These microtubes were prepared by dipping straight lengths of stainless steel wire into aqueous silk fibroin, where the addition of poly(ethylene oxide) (PEO) enabled control of microtube porosity. The microtube properties were characterized in terms of pore size, burst strength, protein permeability, enzymatic degradation, and cell migration. Low porosity microtubes demonstrated superior mechanical properties in terms of higher burst pressures, but displayed poor protein permeability; whereas higher porosity tubes had lower burst strengths but increased permeability and enhanced protein transport. The microtubes also exhibited cellular barrier functions as low porosity tubes prevented outward migration of GFP-transduced HUVECs, while the high porosity microtubes allowed a few cells per tube to migrate outward during perfusion. When combined with the biocompatible and suturability features of silk fibroin, these results suggest that silk microtubes, either implanted directly or preseeded with cells, are an attractive biomaterial for microvascular grafts.

Keywords

Silk fibroin; vascular grafts; arterial tissue engineering; porosity; endothelial cells; bioreactor

1. Introduction

Peripheral arterial disease currently afflicts approximately eight million Americans [1], a number expected to rapidly increase as the population ages and becomes more susceptible to

* Corresponding author. Department of Biomedical Engineering, Tufts University, 4 Colby St., Medford, MA 02155, USA. Tel.: +1-617-627-3251; fax: +1-617-627-3231,. E-mail address: E-mail: David.Kaplan@tufts.edu (D.L. Kaplan).

cardiovascular disease. Currently, more than 450,000 coronary artery bypass graft procedures are performed each year [2]. The 'gold standard' of care in these cases is autologous grafting, where a suitable vein or artery from another site of the body (typically a lower limb or the internal mammary artery) is removed and used to bypass the diseased vein or artery. However, in cases where the patient has a particularly complex arterial disease, has previously failed endovascular procedures, or does not have suitable vessels to harvest, synthetic or tissue-engineered vessels may provide an alternative [3].

Attempts to engineer artificial vessels using natural (e.g., collagen gels and acellularized vessels) or synthetic materials have achieved only modest success [4]. Clinically, two of the more successful synthetic vascular graft materials are expanded polytetrafluoroethylene (ePTFE, Teflon®) and polyethylene terephthalate (PET, Dacron®) [5]. When modified with an anticoagulant such as heparin, or seeded with endothelial cells to generate a tissue-engineered vessel, these synthetic graft materials approach the 'gold standard' of 75% for 5-year patency of autologous vein grafts in human trials [3,6,7]. These results, however, were only achieved for relatively larger diameter grafts (6 to 7 mm inner diameter, ID). When synthetic materials such as unmodified PTFE are used as a microvascular graft for vessels less than 1 mm in diameter, the patency rate drops below this 'gold standard' [8]. In fact, while heparin-bonded ePTFE macrovascular grafts are commercially available in Europe and have recently been approved by the U.S. Food & Drug Administration [9], no microvascular graft (natural, synthetic, or tissue-engineered) has been fully accepted into routine clinical practice, leaving significant room for improvement in the field [10,11].

We propose the use of silk fibroin microtubes as small-caliber (<6 mm ID) blood vessel surrogates. Silk fibroin, derived from *Bombyx mori* silkworm cocoons, is well-characterized and widely used in other biomedical applications, particularly as sutures [12]. This protein is biocompatible, degrades slowly in the body, is readily modified into a variety of formats and generates mechanically robust materials [12]. These properties, in addition to compliance, variable size, good suture retention, low thrombogenicity, and non-toxicity and -immunogenicity, among others, represent the qualities of an ideal blood vessel substitute [3]. Recent processing methods developed in our laboratory allow for the manufacture of microtubes of varying inner diameter, porosity, mechanical strength, and diffusivity. These properties were experimentally verified via SEM imaging, mechanical testing, enzymatic degradation, and protein diffusion measurements. The biocompatibility and efficacy of the silk microtubes as a microvessel surrogate were then evaluated *in vitro* by monitoring the perfusion and migration of endothelial cells through the silk microtube and into a surrounding collagen gel.

2. Materials and methods

2.1. Preparation of aqueous silk fibroin solutions

A 6–8% (w/v) silk fibroin aqueous solution was obtained from *Bombyx mori* silkworm cocoons using previously described procedures [13,14]. Briefly, the silkworm cocoons (supplied by Tajima Shoji Co., LTD., Yokohama, Japan) were extracted in 0.02 M sodium carbonate solution, rinsed in distilled water, dissolved in 9.3 M lithium bromide, and dialyzed against distilled water using a Slide-a-Lyzer dialysis cassette (molecular weight cutoff MWCO, 3,500, Pierce, Rockford, IL) for 48 hours. The resulting 6–8% (w/v) fibroin solution was then concentrated by dialyzing against 10 wt% poly(ethylene glycol) (PEG) to produce a 20–30% (w/v) silk fibroin aqueous solution. All silk fibroin solutions were stored at 4°C until used to make silk microtubes.

2.2. Preparation of silk microtubes

Silk microtubes were prepared by dipping stainless steel wire (0.025” (0.64 mm) diameter, Type 304V, Small Parts, Miami Lakes, FL) into 20–30% (w/v) silk fibroin. When the stainless steel rods were evenly coated with concentrated silk fibroin, they were then dipped into methanol, inducing a transformation in the concentrated silk fibroin from an amorphous liquid to the β-form silk fibroin conformation, characterized by anti-parallel β-sheets [15]. The process of alternate dipping in concentrated aqueous silk fibroin solution and methanol was carried out until the stainless steel wire was evenly coated (2–4 times). The silk-coated wire was then left to dry overnight before being cut at each end and placed in a surfactant solution to remove the silk microtube from the steel wire. Silk tubes of differing size were made according to the same procedure by simply by using larger or smaller stainless steel wire or rod. In this study, the diameters of wire or rod used were 127 μm, 500 μm, 1 mm, 2 mm, 3.2 mm, 4 mm, 5 mm, and 6 mm, producing silk tubes with these approximate inner diameters. Prior to any cell-based experiments, the microtubes were sterilized by briefly soaking in 70% ethanol.

2.3. Preparation of porous silk microtubes

Concentrated silk fibroin solutions were blended with varying volumes of 6 wt% poly(ethylene oxide) (PEO) as we have described previously [16] to form blend ratios of silk fibroin/PEO of 100/0, 99/1, 98/2, 90/10, and 80/20 (wt %). The silk fibroin/PEO blends were gently mixed at room temperature using a spatula before sonication for 10 minutes. Silk/PEO microtubes were made using the same dipping technique and dried overnight as described above. After drying, silk/PEO tubes were immersed in distilled water for 24 hours at room temperature, facilitating the extraction of the PEO phase from the silk/PEO microtube, leaving a porous silk microtube.

2.4. Bioreactor design

In order to assess the performance of silk microtubes in terms of protein permeability and endothelial cell biocompatibility, a simple bioreactor system was developed with the capability to culture and image three microtubes (Figure 1). The bioreactor consisted of a glass cover slip (Goldseal, No. 1, 24 × 60 mm, Ted Pella, Redding, CA) irreversibly bonded using vacuum gas plasma to a PDMS (Sylgard 184, Ellsworth Adhesives, Germantown, WA) casting, forming three independent medium wells. The mold for the PDMS casting was machined from a polycarbonate block using a small CNC mill (MDX-15, Roland ASD, Lake Forest, CA). The overall dimensions of the PDMS casting were 6.0 cm × 2.5 cm × 1.0 cm, with 3 wells of dimension 1.0 cm × 1.5 cm each. In the center of each well, a stainless steel rod (0.025” diameter, Type 304V, Small Parts, Miami Lakes, FL) was positioned approximately 500 μm from the bottom edge of the bioreactor and embedded in the PDMS during the pouring and curing process. This rod served as a space holder for hypodermic, stainless steel needles (23-gauge, BD, Franklin Lakes, NJ) that were later used to perfuse the microtubes. Pharmed tubing (0.51 mm inner diameter, Cole-Parmer, Vernon Hills, IL) was used to perfuse the bioreactor using a syringe pump (Harvard Apparatus, Holliston, MA). Microtubes were embedded in a collagen gel matrix in order to mimic *in vivo* implantation conditions and to allow comparison with previously reported studies on the formation of microvascular tubes [17].

2.5. Preparation of collagen gels

Collagen gels were prepared based on a previously developed method [18] with minor changes. Collagen gels were prepared on ice by mixing 1.22 mL type I rat tail liquid collagen (~4 mg/mL in 0.02 N acetic acid, Upstate Cell Signaling Solutions, Lake Placid, NY), 12.2 μL 2M sodium hydroxide, 20 μL 100 mM ascorbic acid, and 768 μL of growth medium [19] for a final collagen concentration of approximately 2.5 mg/mL. This collagen suspension was then aliquoted in 400 μL volumes into each well of the bioreactor and maintained at 25°C for 15–

30 minutes to allow for even gelation before being placed in the incubator. For long-term experiments, 200 μL of growth medium was added to the top of each gel after 1–2 hours.

2.6. Imaging of silk microtubes – SEM and confocal microscopy

Scanning electron microscopy (SEM) was used to determine the pore size distribution in the silk microtubes. Silk microtube samples were sputter coated with gold using a Polaron SC502 Sputter Coater (Fisons, VG Microtech, East Sussex, England) and imaged using a JEOL JSM-840 Scanning Microscope (JEOL Ltd., Tokyo, Japan). The SEM images, along with image analysis software (ImageJ, National Institutes of Health, USA) were used to determine the mean pore size of the silk microtubes.

Fluorescence images of the silk microtubes within the bioreactor were acquired using a Leica DMIRE2 confocal microscope with a TCS SP2 scanner (Leica Microsystems, Mannheim/Wetzlar, Germany).

2.7. Characterization of silk microtubes – FT-IR, burst strength, protein permeability, and enzymatic degradation

The infrared spectra of the silk fibroin and silk fibroin/PEO microtubes were measured using a Bruker Equinox 55/S FT-IR spectrometer. Samples were taken using hydrated microtubes, with each spectrum acquired over the range of 4000-400 cm^{-1} for 66 scans with a resolution of 4 cm^{-1}.

The burst strength of the silk microtubes were measured by cannulating the hydrated silk tubes, cut to approximately 1 cm lengths, and filling the tubes at a rate of 0.4 mL/min with water. Silk microtubes were submerged in water during perfusion. Pressure inside the tube was increased by blocking flow out of one end of the tube and recorded using a digital manometer (Sper Scientific, Scottsdale, AZ) until tube failure, with the observed maximum pressure logged.

Protein diffusion through the silk microtubes was assessed by perfusing the silk microtubes embedded within an acellular collagen gel in the bioreactor system with a solution of Alexa-Fluor-488-labeled BSA (50 μg/mL in media, Molecular Probes, Eugene, OR). Fluorescence images were acquired every minute for 20 minutes using confocal microscopy and the apparent permeability coefficient was calculated according to previously described techniques [17,20]. Briefly, the permeability coefficient P was calculated from the equation $P = (1/I_0)\,(dI/dt)_0\,(r/2)$, where I_0 is the fluorescent intensity of the image outside of the tube at time zero, $(dI/dt)_0$ is the initial rate of increase in intensity as BSA diffuses out of the tube, and r is the tube radius. Image intensities were measured using Leica confocal software, with $(dI/dt)_0$ estimated by plotting the image intensity outside of the tube versus time over the first 4 minutes of diffusion and calculating the slope (LCS Lite, Leica Microsystems, Mannheim/Wetzlar, Germany).

Silk microtubes were assessed for enzymatic degradation over time using a protocol described previously [21]. Briefly, silk microtubes (1 cm in length, N=3 per group and time point) were incubated in 1 mL of 1.0 mg/mL Protease XIV (5.3 units/mg, Sigma-Aldrich, St. Louis, MO) in PBS or in PBS as a negative control at 37°C for a period of ten days. Solutions were changed daily and samples were taken every 3–4 days. Samples were washed once with PBS before drying overnight in a laminar flow hood. Samples were weighed and compared to their initial weight.

2.8. Cell culture

Human umbilical vein endothelial cells (HUVECs) were cultured according to company protocols. Briefly, HUVECs (Cambrex, Walkersville, MD) were grown in optimized growth

media (EGM-2) consisting of Endothelial Basal Medium-2 supplemented with EGM-2 Bullet kit (Cambrex), along with 100 U/mL penicillin, 1000 U/mL streptomycin, and 0.2% fungizone antimycotic (GIBCO, Carlsbad, CA). Cells were cultured at 37°C, 5% CO_2/95% air, and 95% relative humidity. Cell culture medium was replenished twice per week, and cells were passaged at approximately 80% confluence using Trypsin-EDTA (0.25% trypsin with 1 mM EDTA•4Na) and frozen in cryogenic media consisting of growth medium supplemented with 8% (v/v) dimethyl sulfoxide (DMSO).

2.9. Generation of green fluorescent protein (GFP) expressing HUVECs

A GFP-expressing line of HUVECs was generated using a previously described lentivirus system [22]. HUVECs were transduced at MOI 1 (multiplicity of infection), with five milliliters of virus-containing supernatant (100,000 virus particles/mL) added to 5×10^5 HUVECs. An additional 5 mL of EGM-2 media was added in the flask along with protamine sulfate (6 μg/ml) to enhance the infection. The cells were incubated for 3 hours with the lentivirus, then washed twice with PBS before adding EGM-2 media. The efficiency of GFP transduction was evaluated through fluorescence microscopy and fluorescence-activated cell sorting (FACS) analysis (BD, Franklin Lakes, NJ). Upon generation of stable GFP-expressing HUVECs (GFP-HUVECs) as given by the presence of fluorescence in the cells over several cell passages, cells were cultured according to standard HUVEC protocol as described above [22].

2.10. Perfusion of silk microtubes with GFP-labeled endothelial cells

To assess cellular migration through the silk microtubes, they were perfused with GFP-HUVECs. The silk microtubes were maintained within an acellular collagen gel in the bioreactor set-up as described above. GFP-HUVECs were maintained and harvested according to the above protocols to a concentration of 5×10^6 cells/mL. This suspension of GFP-HUVECs was then perfused using a remote push-pull syringe pump (Harvard Apparatus, Holliston, MA), programmed to flow at a rate of 4 μL/min into the bioreactor for 2.5 hours before reversing perfusion and flowing at the same rate in the opposite direction. This perfusion kept the GFP-HUVECs flowing within the microtube in a back-and-forth manner, over the course of three days. Permeability of the silk microtubes to GFP-HUVECs was assessed using confocal microscopy.

2.11. Statistical analysis

All assays were repeated with a minimum sample size of N=3. Experimental groups for the pore size and burst pressure data were compared using a two-sample t-test for pair-wise comparisons using Minitab 15 statistical software (State College, PA). Statistically significant values were defined as $p < 0.05$.

3. Results and discussion

3.1. Silk microtube fabrication – Controlling pore size distribution and protein structure

Silk tubes were manufactured using layer-by-layer deposition of concentrated silk fibroin on a stainless steel rod of defined diameters, using methanol to induceβ-sheet formation to provide stability in aqueous solution and improved mechanical properties [15]. This technique provided solid silk tubes of low pore size distribution and low porosity, restricting nutrient and oxygen diffusion through the walls of the microtubes. To improve these diffusion properties, porous, three-dimensional silk tubes were generated by adding various fractions of PEO to the concentrated silk fibroin (as described in the materials section). By varying the specific weight percent of PEO, defined pore sizes were obtained, with greater weight percentages of PEO creating tubes with larger pore sizes. This provides a measure of control over the microtube permeability.

Silk microtubes were analyzed for surface pore size distribution and roughness at the exterior surface as well as the cross-section of the microtube using SEM. As shown in Figure 2, pore size distributions in the silk microtubes can be controlled by using different weight percentages of PEO. These pore sizes range from the smooth, uniform surface of the 100% silk fibroin microtubes to the rough, highly-porous microtubes composed of the 90/10 wt % silk/PEO or 80/20 wt % silk/PEO blends. Intermediate porosities were achieved using lower weight percentages of PEO (Figure 2b,c). Surface pore size distribution increased as the weight percentage of PEO increased (Figure 3), which agrees with our previously reported results for 2-D films generated from silk/PEO blends [16]. For the 3-D microtubes, despite similar mean pore size distribution values for 10 and 20 wt % PEO, large void spaces were more prevalent at the higher PEO concentration. As reported below, this increased void fraction likely accounts for decreased mechanical robustness and burst strength of 80/20 wt % silk/PEO blends. This ability to alter microtube pore size distribution creates opportunities to tailor microtube manufacture to specific applications, e.g. high porosity tubes for applications where high transport rates, but not mechanical strength, are needed versus low porosity tubes where mechanical integrity, but not transport, is critical.

The presence of beta-sheets in all formulations of silk fibroin and silk fibroin/PEO microtubes was confirmed using FT-IR (Figure 4). Each microtube demonstrated a predominantly β-sheet structure (1697 cm-1, 1626 cm-1, amide I; 1526 cm-1, amide II), which was induced by the methanol treatment applied to all microtubes. There were no differences in the amide I and amide II spectral bands between microtubes of pure silk fibroin and those of silk/PEO blends, agreeing with previously reported structural data using silk fibroin and PEO films [16].

3.2. Mechanical strength of silk microtubes

The burst pressure of the silk microtubes was a function of pore size distribution, with silk microtubes with smaller pore sizes (100/0, 99/1, and 98/2 wt % silk fibroin/PEO) demonstrating higher burst pressures than those with larger pores (90/10 and 80/20 wt % silk fibroin/PEO) (Figure 5). Burst pressures for the microtubes of lower porosities were very high, with average burst pressure values of 2780±876 mm Hg, 2470±937 mm Hg, and 2460±844 mm Hg for 100/0, 99/1, and 98/2 wt % silk fibroin/PEO, respectively. While these burst pressures are from smaller caliber vessels, it is worth noting that these burst strengths are significantly higher than those of human saphenous veins (1680±307 mm Hg), the current gold standard for bypass grafts [23], and are also higher than reported burst strengths for electrospun silk tubes (811±77.2 mm Hg) [24]. Burst strengths of 90/10 and 80/20 wt % silk fibroin/PEO tubes were significantly lower than those values for the tubes with the smaller pore sizes, with values of 680±327 mm Hg and 10±2 mm Hg, respectively. Compared to physiological pressures of approximately 100–140 mm Hg (coronary artery during systole) or 15–40 mm Hg (capillary blood pressure) [4,25], most microtubes failed above this level, indicating feasibility for future *in vivo* studies involving tubes manufactured with greater than (or equal to) 90/10 wt % silk fibroin/PEO blends. Microtubes typically failed by developing a leak at one end of the microtube, though occasionally failed by developing a pinhole leak. As indicated by their burst pressures, the low pore size tubes were mechanically robust when compared to the microtubes with larger pore sizes, which were often weak and difficult to cannulate without splitting the tube.

3.3. Protein permeability of silk microtubes

Silk microtube permeability was measured by perfusing the tubes with Alexa-Fluor-488-labeled BSA while embedded in an acellular collagen gel. Using fluorescent confocal microscopy, time-lapse images were taken every minute over a 20-minute perfusion time for microtubes manufactured with different silk fibroin/PEO ratios. These images indicated that there is an increase in microtube permeability as the pore size distribution in the microtubes is increased, due to the use of higher concentrations of PEO in the microtube production (Figure

6). Silk (100% fibroin) microtubes exhibited a strong barrier function, allowing little to no perfusion of BSA through the tubes over the course of the 20-minute perfusion time. Labeled BSA was clearly visible perfusing through the silk microtube due to the optical clarity of the microtube.

Microtubes with increasing PEO concentrations were more opaque, eliminating this visual identification of labeled BSA within the silk microtube. These fibroin/PEO microtubes, with their increased pore sizes, demonstrated diffusion of the labeled BSA from the microtubes and into the collagen gel. The apparent permeability coefficient of these porous tubes were estimated to be $1.1\times10^{-5}\pm7.6\times10^{-6}$, $7.3\times10^{-4}\pm1.5\times10^{-4}$ cm/s, $7.3\times10^{-4}\pm0.55\times10^{-4}$ cm/s, and $9.4\times10^{-4}\pm1.9\times10^{-4}$ cm/s for 99/1, 98/2, 90/10, and 80/20 wt % silk fibroin/PEO microtubes (n=3), respectively. The tubes with small pore sizes (99/1 wt % silk fibroin/PEO) had a permeability coefficient that was an order of magnitude lower than those of the tubes with large pore sizes and was also comparable to values achieved using endothelial cell-lined microvascular tubes embedded in collagen [17]. In these acellular experiments, after twenty minutes of perfusion, the collagen gel was near saturation for the 90/10 and 80/20 wt % silk fibroin/PEO microtubes, consistent with their larger sized pore distribution.

3.4. Enzymatic degradation of silk microtubes

Silk microtubes were subjected to an *in vitro* proteolytic digest over the course of ten days to track degradation over time. Protease (Protease XIV) was chosen based on previously reported results on the degradation of silk fibroin fibers [21]. For silk fibroin microtubes, degradation was observed in all silk samples incubated in the protease solution, demonstrating a general linear degradation rate in terms of weight ratio based on the sample mass at each time point divided by initial microtube mass (Figure 7). At each progressive time point, silk microtubes were considerably more brittle, demonstrating a loss of mechanical integrity as they degraded by gross observation. Control samples incubated in PBS did not exhibit any mass loss and were observed to be typical in terms of microtube integrity at all time points. Interestingly, silk microtube degradation was not dependent on microtube permeability as all microtubes displayed a similar linear trend. This may be due to the methanol treatment used in all formulations of silk tubes, creating theβ-sheet structure discussed previously in all tubes, or the relatively small tube sizes used (~ 1 cm length) which may mask the effects of porosity. It should be noted that while considerable biodegradability and losses in mechanical integrity were observed in this *in vitro* study, prior work has found degradation rates of silk fibroin were diminished *in vivo* [12]. This suggests that *in vivo* implantation of the silk microtubes may result in slower degradation rates than what was observed here *in vitro*. Furthermore, additional steps such as additional dipped layers of silk fibroin when making the microtubes or pre-conditioning the tubes with endothelial cells may slow degradation to the point where the rate of extracellular matrix being deposited by the cells matches or exceeds the degradation rate of the silk tube itself. This represents the ideal case where the scaffold gradually becomes a fully-integrated tissue.

3.5. Cellular permeability of silk microtubes

Silk microtubes of all pore size distributions limited migration of HUVECs over the course of a three day perfusion. Either no cells, or only a few GFP-transduced HUVECs per microtube, were detected outside in the surrounding collagen gel (Figure 8). A high concentration (5×10^6 cells/mL) of GFP-HUVECs was used in order to easily detect perfusion and migration of the cells through the microtubes, with cells imaged through the use of fluorescent confocal microscopy. Images throughout the microtube were taken after three hours and three days of perfusion. As in the protein diffusion experiments, GFP-HUVECs were only visible in the lumen of the tubes at the highest concentration of silk (100% fibroin and 99/1% fibroin/PEO). These tubes exhibited the strongest barrier function for endothelial cells, as none were found

to migrate into the collagen gel. Microtubes of higher permeability, however, demonstrated limited cell migration into the collagen gel, typically at a rate of a few cells per tube over the three day perfusion. Taken together with the protein diffusion data, the microtubes demonstrate the ability to selectively allow protein diffusion through the microvascular graft, while largely preventing any cell migration. This ability to reduce cellular migration, even in the case of highly porous tubes, suggests the potential for these microtubes to be pre-endothelialized prior to implantation as a microvascular graft in future studies, a technique often considered to be critical for the prevention of thrombosis in tissue-engineered vascular grafts [2].

3.6. Silk microtubes with different diameters

In order to demonstrate the general applicability of this technique towards microvascular grafting, tubes were manufactured in a range from 100 μm ID to 6 mm ID, the generally reported maximum diameter to be considered a microvascular graft. The dipping technique allows tubes to be formed with different diameters quickly and easily, as opposed to other silk-based techniques such as electrospinning, which requires optimization of multiple processing steps (e.g. mandrel selection, voltages, etc.) [24]. Tubes of approximately 127 μm, 500 μm, 1 mm, 2 mm, 3.2 mm, 4 mm, 5 mm, and 6 mm ID were successfully generated using the dipping technique (Figure 9), although those larger than 2 mm ID were occasionally subject to cracking as the silk dried around the stainless steel wire or rods after methanol treatment.

An important feature of the process is the all aqueous solution used during vessel formation. This would allow the incorporation of labile molecules or therapeutics into the coatings with retention of bioactivity, as we have previously shown for BMP-2 [14]. We have previously shown that the methanol used in the process, to induce beta sheet formation and thus stability in water, can be replaced with a nitrogen gas drying step [26], a useful option to functionalize these new microvessels with therapeutics. Notably, this can all be done in the context of matching silk tube design specifications to specific applications, creating a good balance between porosity, transport properties, mechanical properties, and tube size. For example, a patient in need of a larger diameter (4–5 mm ID) graft can be manufactured a silk tube of this exact inner diameter, with low porosity (as transport is not critical at that size), and definable wall thickness (controlled by number of dips in silk fibroin) based on some measure of the required mechanical load on the graft (e.g. blood pressure). This kind of versatility position these silk microtubes as a potentially powerful new method of creating microvascular grafts for applications in medicine and tissue engineering.

4. Conclusion

The ability to form small tubes (0.1 to 6.0 mm ID) with controllable pore sizes with silk fibroin aqueous solution suggest that these tubes may offer a novel option for microvascular grafts. Tube properties can be tailored through the addition of various concentrations of polyethylene oxide (PEO) to silk fibroin before forming the silk microtubes through a simple dipping technique and leaching out the PEO to generate the porous silk microtubes. Recent reports have suggested the need for porous scaffolds for vascular tissue engineering applications [27], and these porous silk microtubes can address this need. The porous silk microtubes were characterized in terms of pore size, burst pressure, protein diffusion, enzymatic degradation, and cell migration. Higher concentrations of silk fibroin (100/0, 99/1 wt % silk fibroin/PEO) produced microtubes that exhibited the lowest pore sizes, highest burst pressures, and strongest barrier function for both protein diffusion and cell migration. Greater concentrations of PEO (90/10, 80/20 wt % silk fibroin/PEO), however, produced the opposite effect as these microtubes had larger pore sizes, lower burst pressures, higher rates of protein diffusion, and occasional cell migration. In between these two extremes, silk tubes of 98/2 wt % silk fibroin/PEO had burst pressures on par with those of 100% silk fibroin microtubes, and also

demonstrated a permeability to small proteins while limiting endothelial cell migration. This type of microtube may represent a useful next step for microvascular grafts since it is capable of withstanding physiological pressures, while also allowing control of protein diffusion and cell migration.

This ability to control properties of the microtubes, combined with their relative ease of manufacture compared to other techniques suggests that these silk microtubes are an attractive option for vascular applications. Future work will seek to further improve the manufacturing process through automation, establishing procedures for more uniform and reproducible microtube formation, a factor critical for *in vivo* applications. As a potential microvascular graft material, these microtubes offer the future benefit of being functionalized via the facile attachment of RGD-peptides and other peptides or proteins as described in our previous work [28]. This chemical modification of the silk would allow for control over the luminal endothelialization of the microtubes, a factor critical for improved patency rates in *in vivo* implantation studies. In terms of future *in vitro* work, these porous microtubes can be used as a means of controlling oxygen and nutrient diffusion to cells embedded in hydrogels using the bioreactor set-up described in this work. Overall, these silk microtubes represent a simple method of controlling critical microvascular properties, offering opportunities for advancement over existing materials in tissue engineering for both *in vivo* and *in vitro* applications.

Acknowledgments

The authors thank Amanda Murphy for her assistance with the FT-IR spectra. We would like to acknowledge funding from the Tissue Engineering Resource Center (TERC) - NIH EB002520 from the National Institute of Biomedical Imaging and Bioengineering.

References

1. Statistical Fact Sheet - Miscellaneous. 2004 [cited November 28, 2006]. Available from: http://www.americanheart.org/presenter.jhtml?identifier=2021
2. Mitchell SL, Niklason LE. Requirements for growing tissue-engineered vascular grafts. Cardiovasc Pathol 2003;12:59–64. [PubMed: 12684159]
3. Baguneid MS, Seifalian AM, Salacinski HJ, Murray D, Hamilton G, Walker MG. Tissue engineering of blood vessels. Br J Surg 2006;93:282–290. [PubMed: 16498591]
4. Isenberg BC, Williams C, Tranquillo RT. Small-diameter artificial arteries engineered in vitro. Circ Res 2006;98:25–35. [PubMed: 16397155]
5. Kannan RY, Salacinski HJ, Sales K, Butler P, Seifalian AM. The roles of tissue engineering and vascularisation in the development of micro-vascular networks: a review. Biomaterials 2005;26:1857–1875. [PubMed: 15576160]
6. Meinhart JG, Deutsch M, Fischlein T, Howanietz N, Froschl A, Zilla P. Clinical autologous in vitro endothelialization of 153 infrainguinal ePTFE grafts. Ann Thorac Surg 2001;71:S327–331. [PubMed: 11388216]
7. Lambert AW, Fox AD, Williams DJ, Horrocks M, Budd JS. Experience with heparin-bonded collagen-coated grafts for infrainguinal bypass. Cardiovasc Surg 1999;7:491–494. [PubMed: 10499890]
8. Harris JR, Seikaly H. Evaluation of polytetrafluoroethylene micrografts in microvascular surgery. J Otolaryngol 2002;31:89–92. [PubMed: 12019749]
9. FDA clears GORE PROPATEN vascular graft. 2006 [cited February 19, 2007]. Available from: http://www.goremedical.com/press/news/propaten-uslaunch2006
10. Bosiers M, Deloose K, Verbist J, Schroe H, Lauwers G, Lansink W, et al. Heparin-bonded expanded polytetrafluoroethylene vascular graft for femoropopliteal and femorocrural bypass grafting: 1-year results. J Vasc Surg 2006;43:313–319. [PubMed: 16476607]
11. Heyligers JM, Verhagen HJ, Rotmans JI, Weeterings C, de Groot PG, Moll FL, et al. Heparin immobilization reduces thrombogenicity of small-caliber expanded polytetrafluoroethylene grafts. J Vasc Surg 2006;43:587–591. [PubMed: 16520178]

12. Altman GH, Diaz F, Jakuba C, Calabro T, Horan RL, Chen J, et al. Silk-based biomaterials. Biomaterials 2003;24:401–416. [PubMed: 12423595]
13. Kim UJ, Park J, Li C, Jin HJ, Valluzzi R, Kaplan DL. Structure and properties of silk hydrogels. Biomacromolecules 2004;5:786–792. [PubMed: 15132662]
14. Li C, Vepari C, Jin HJ, Kim HJ, Kaplan DL. Electrospun silk-BMP-2 scaffolds for bone tissue engineering. Biomaterials 2006;27:3115–3124. [PubMed: 16458961]
15. Jin HJ, Kaplan DL. Mechanism of silk processing in insects and spiders. Nature 2003;424:1057–1061. [PubMed: 12944968]
16. Jin HJ, Park J, Valluzzi R, Cebe P, Kaplan DL. Biomaterial films of Bombyx mori silk fibroin with poly(ethylene oxide). Biomacromolecules 2004;5:711–717. [PubMed: 15132651]
17. Chrobak KM, Potter DR, Tien J. Formation of perfused, functional microvascular tubes in vitro. Microvasc Res 2006;71:185–196. [PubMed: 16600313]
18. Lewus KE, Nauman EA. In vitro characterization of a bone marrow stem cell-seeded collagen gel composite for soft tissue grafts: effects of fiber number and serum concentration. Tissue Eng 2005;11:1015–1022. [PubMed: 16144437]
19. Wang Y, Kim UJ, Blasioli DJ, Kim HJ, Kaplan DL. In vitro cartilage tissue engineering with 3D porous aqueous-derived silk scaffolds and mesenchymal stem cells. Biomaterials 2005;26:7082–7094. [PubMed: 15985292]
20. Huxley VH, Curry FE, Adamson RH. Quantitative fluorescence microscopy on single capillaries: alpha-lactalbumin transport. Am J Physiol 1987;252:H188–197. [PubMed: 3492924]
21. Horan RL, Antle K, Collette AL, Wang Y, Huang J, Moreau JE, et al. In vitro degradation of silk fibroin. Biomaterials 2005;26:3385–3393. [PubMed: 15621227]
22. Rubinson DA, Dillon CP, Kwiatkowski AV, Sievers C, Yang L, Kopinja J, et al. A lentivirus-based system to functionally silence genes in primary mammalian cells, stem cells and transgenic mice by RNA interference. Nat Genet 2003;33:401–406. [PubMed: 12590264]
23. L'Heureux N, Paquet S, Labbe R, Germain L, Auger FA. A completely biological tissue-engineered human blood vessel. Faseb J 1998;12:47–56. [PubMed: 9438410]
24. Soffer L, Wang X, Kluge J, Dorfmann L, Kaplan D, Liske G. Silk-based electrospun tubular scaffolds for tissue-engineered vascular grafts. J Biomater Sci. Submitted
25. Williams SA, Wasserman S, Rawlinson DW, Kitney RI, Smaje LH, Tooke JE. Dynamic measurement of human capillary blood pressure. Clin Sci (Lond) 1988;74:507–512. [PubMed: 3370917]
26. Wang X, Kim HJ, Xu P, Matsumoto A, Kaplan DL. Biomaterial coatings by stepwise deposition of silk fibroin. Langmuir 2005;21:11335–11341. [PubMed: 16285808]
27. Sarkar S, Lee GY, Wong JY, Desai TA. Development and characterization of a porous micro-patterned scaffold for vascular tissue engineering applications. Biomaterials 2006;27:4775–4782. [PubMed: 16725195]
28. Sofia S, McCarthy MB, Gronowicz G, Kaplan DL. Functionalized silk-based biomaterials for bone formation. J Biomed Mater Res 2001;54:139–148. [PubMed: 11077413]

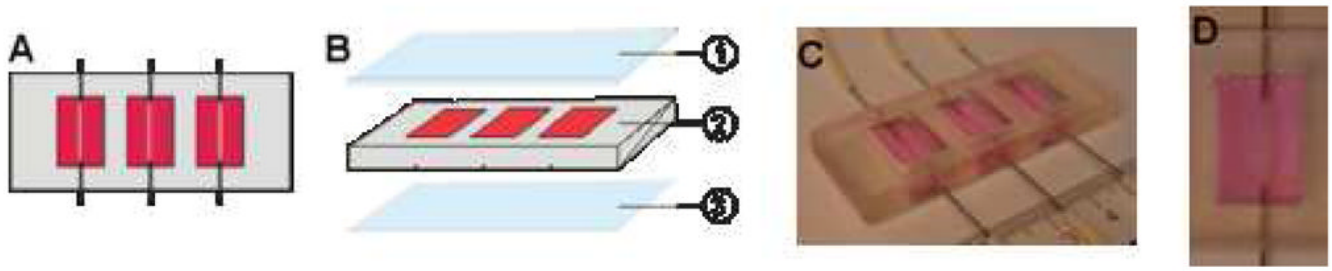

Figure 1.

Bioreactor schematic. (A) Three bioreactors of dimension 10 mm × 15 mm × 5 mm are arranged within a 25 mm × 60 mm × 5 mm PDMS block, with 15 mm center-to-center spacing between each bioreactor. Each bioreactor is perfused by 23G stainless steel needles. The needles are spanned by silk microtubes (500 μm inner diameter) and are perfused at a rate of 4 μL/min. The needles are approximately 500 μm from the cover glass to allow for confocal imaging. (B) The devices are assembled from layers of PDMS and glass consisting of a glass slide (1), a bioreactor layer (2), and a glass cover slip (3). The glass cover slip is attached via plasma treatment and the glass slide is attached using label tape. (C) Image of bioreactor. (D) Image of single well with silk tube and collagen gel.

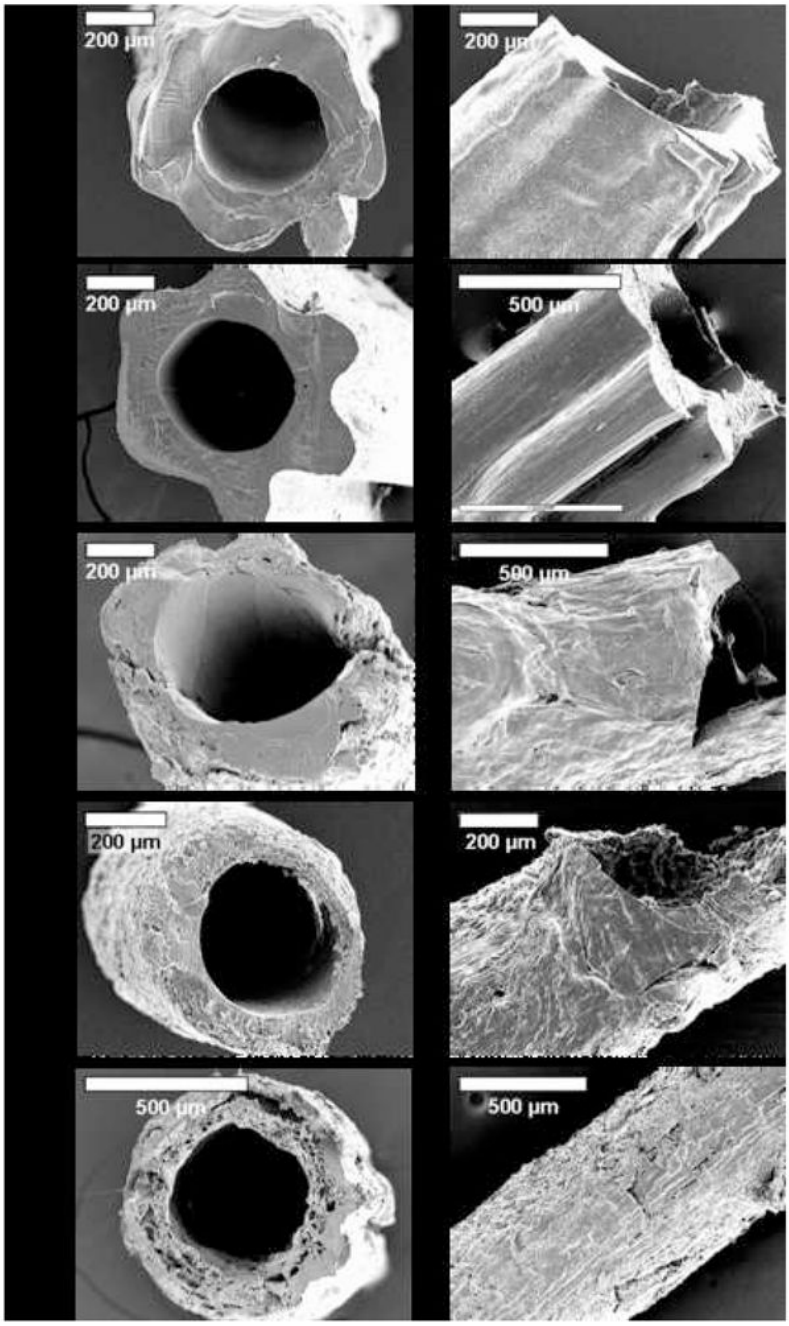

Figure 2.
SEM images of microtubes of silk fibroin and silk fibroin/PEO blends: (A) silk fibroin, (B) 99/1 wt %, (C) 98/2 wt %, (D) 90/10 wt %, (E) 80/20 wt % (silk fibroin/PEO).

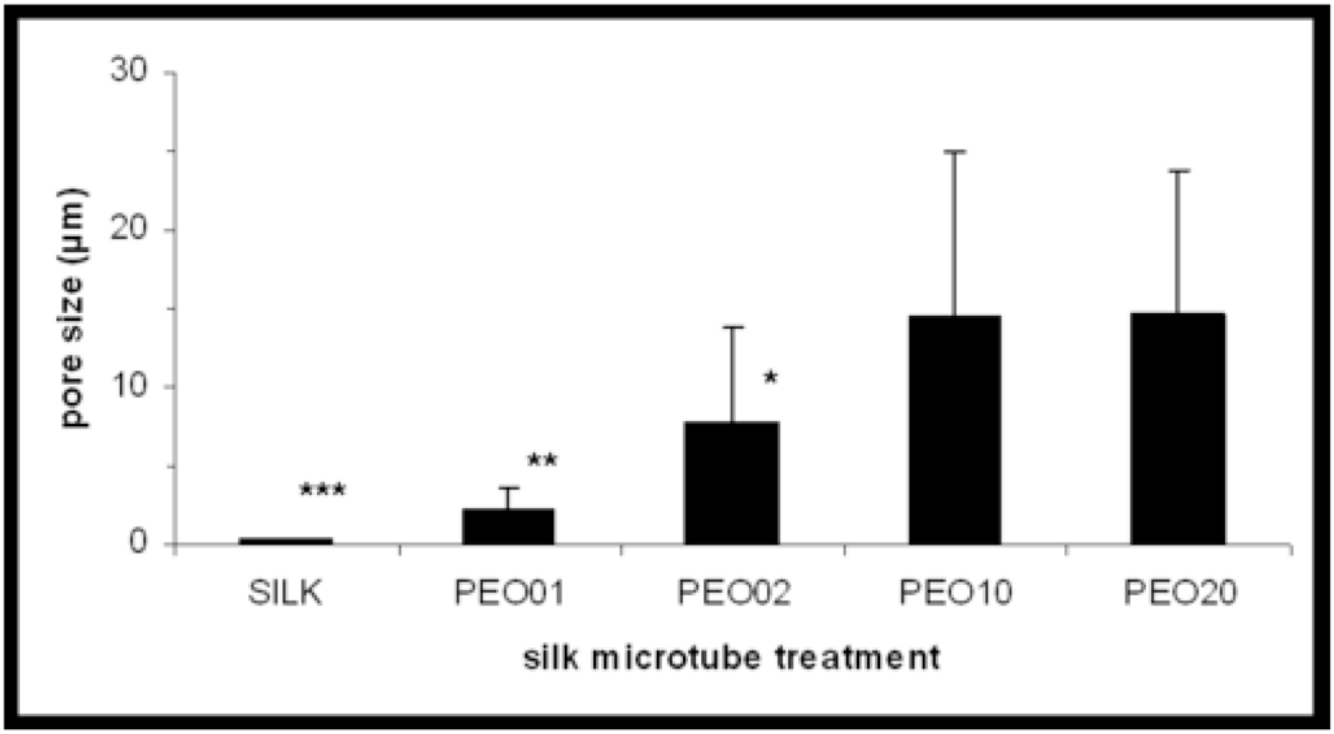

Figure 3.

Pore sizes (μm) of silk fibroin/PEO blend microtubes as a function of microtube treatment. Surface pore sizes of the silk microtubes of different silk fibroin/PEO blends were measured and quantified both along the tube surface and cross-section using SEM images and ImageJ software. Microtube treatments are given either as 100% silk fibroin (SILK) or according to wt % of PEO in a silk fibroin/PEO blend (e.g. PEO01 represents a 99/1 wt % silk fibroin/PEO blend). * indicates P<0.01 with PEO10, PEO20; ** indicates P<0.01 with PEO02, PEO10, PEO20; *** indicates P<0.01 with PEO01, PEO02, PEO10, PEO20 (two-sample t-test).

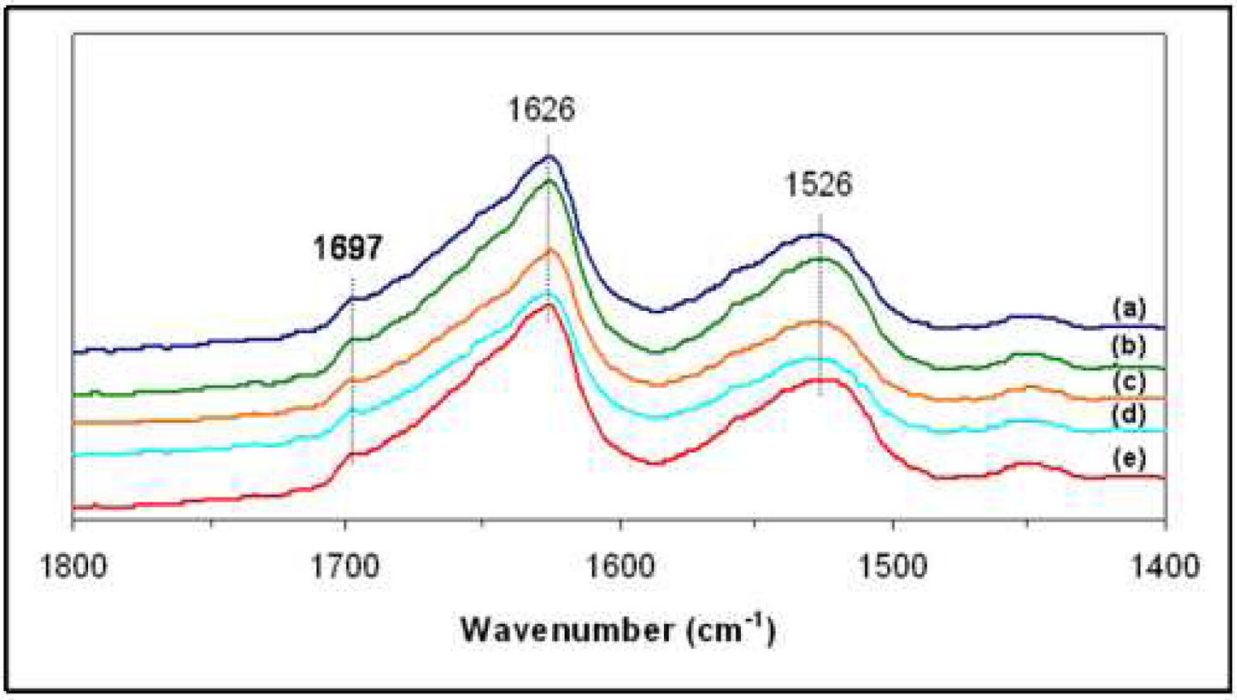

Figure 4.
FT-IR spectra of microtubes of silk fibroin and silk fibroin/PEO blends: (a) silk fibroin, (b) 99/1 wt %, (c) 98/2 wt %, (d) 90/10 wt %, (e) 80/20 wt % (silk fibroin/PEO).

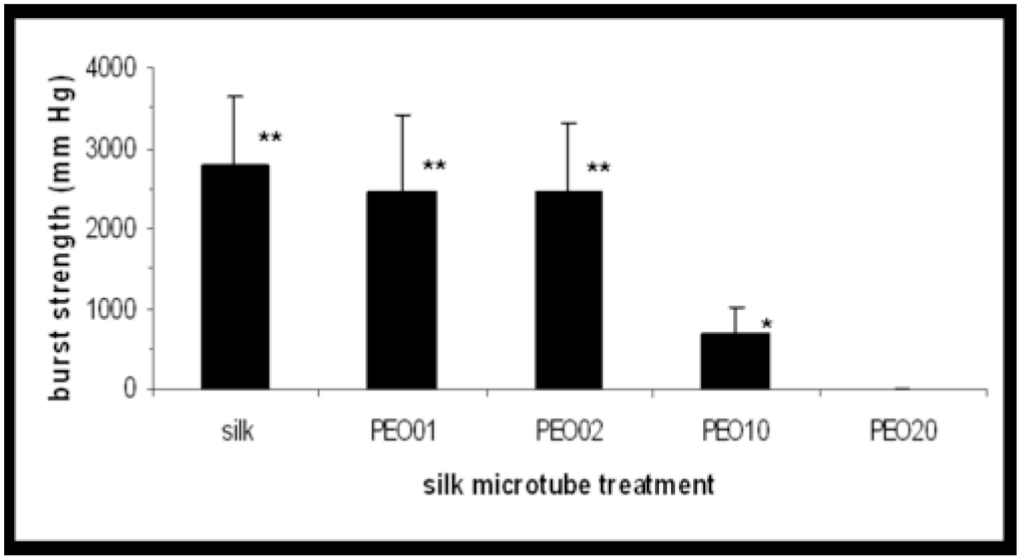

Figure 5.

Burst pressure of silk microtubes as a function of microtube treatment. Internal pressure of the microtubes was increased by flowing water through the microtube, keeping one end of the flow loop closed. Pressure at point of failure was recorded with a digital manometer (n=5–6). * indicates $P<0.05$ with PEO20; ** indicates $P<0.01$ with PEO10, PEO20 (two-sample t-test).

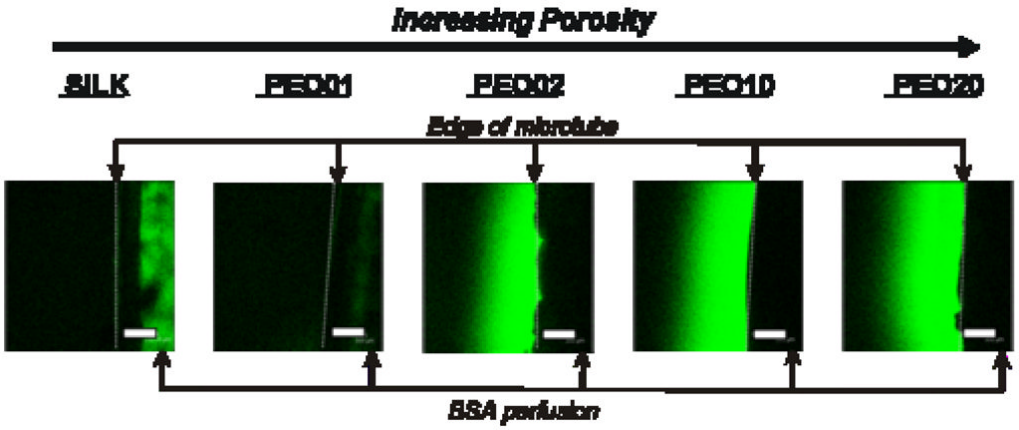

Figure 6.

Permeability of silk microtubes as a function of tube porosity. Silk microtubes embedded in a collagen gel were perfused with labeled BSA, and fluorescent confocal microscopy images are shown after 10 minutes of perfusion. Edges of microtubes are shown at the right of each image with labeled BSA diffusing out to the left of the microtube (edge of microtube given by dashed line). Labeled BSA can be seen perfusing through the middle of the 100% silk fibroin tube and is faintly visible in the PEO01 tube. Labeled protein is not visible in the middle of silk microtubes with greater percentages of PEO due to the opaqueness of the tubes. Scale bars = 300 microns.

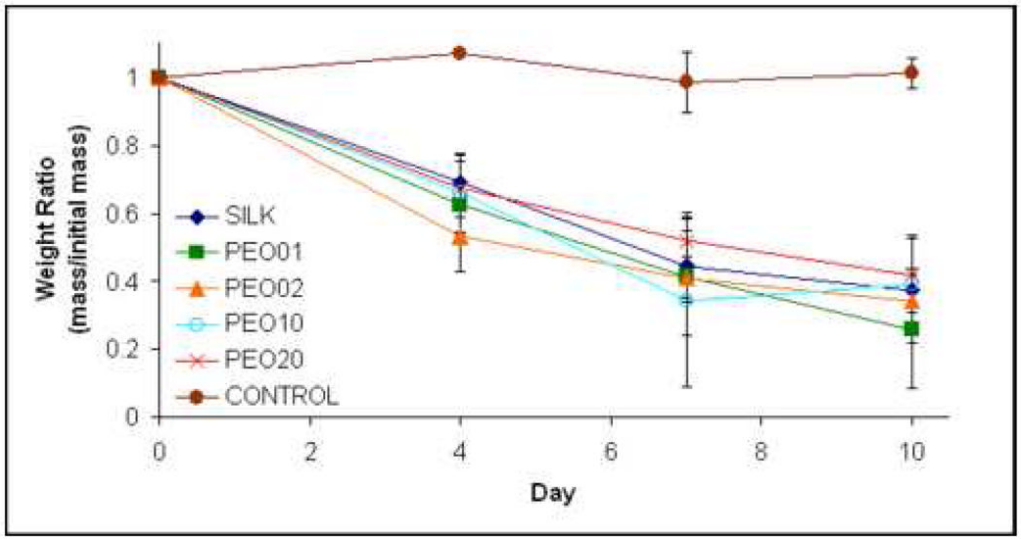

Figure 7.
Enzymatic degradation of silk microtubes. Silk microtubes were degraded over time in 1.0 mg/mL protease or in PBS (control). Data is reported as a weight ratio of microtube mass on day of sampling divided by initial mass of microtube.

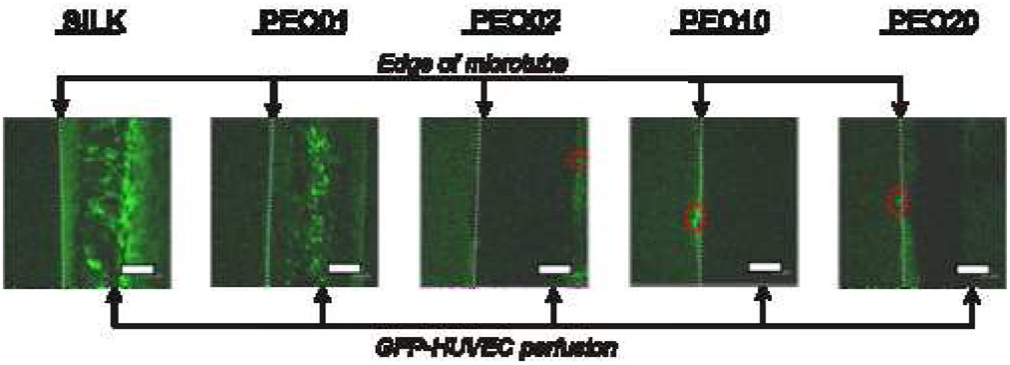

Figure 8.

Perfusion of GFP-transduced human umbilical vein endothelial cells (HUVECs). Silk microtubes embedded in a collagen gel were perfused with green fluorescent protein (GFP) transduced HUVECs. GFP-HUVECs were perfused back and forth at a rate of 4 μL/min through the silk microtubes using a syringe pump, and fluorescent confocal microscopy images are shown after 3 days of perfusion. Sections of the microtubes are shown at the right of each image with GFP-HUVECs present in the channel of the microtube (edge of microtube given by dashed line). These cells are visible in the 100% silk fibroin and PEO01 tubes, but their presence in the microtubes with greater percentages of PEO is obscured due to the opaqueness of the tubes. The silk microtubes were a significant barrier to cell migration. At low porosity, GFP-HUVEC migration was completely blocked; at higher porosities (PEO10 and PEO20) cell migration was limited to a few cells (outlined by red-dashed ovals) over the entire microtube. Scale bars = 300 microns.

Figure 9.
Silk microtubes at a range of diameters. Stainless steel wire and rods were used to generate silk tubes with approximate inner diameters of (from left to right): 127 μm, 500 μm, 1 mm, 2 mm, 3.2 mm, 4 mm, 5 mm, and 6 mm. This demonstrates that these silk microtubes can be easily generated for any size microvascular graft (<6 mm inner diameter).